Circulation

American Heart Association®

Learn and Live ℠

Early Onset and Progression of Left Ventricular Remodeling After Alcohol Septal Ablation in Hypertrophic Obstructive Cardiomyopathy

Willem G. van Dockum, Aernout M. Beek, Folkert J. ten Cate, Jurrien M. ten Berg, Olga Bondarenko, Marco J.W. Götte, Jos W.R. Twisk, Mark B.M. Hofman, Cees A. Visser and Albert C. van Rossum

The online version of this article, along with updated information and services, is located on the World Wide Web at:

http://circ.ahajournals.org/content/111/19/2503

Early Onset and Progression of Left Ventricular Remodeling After Alcohol Septal Ablation in Hypertrophic Obstructive Cardiomyopathy

Willem G. van Dockum, MD; Aernout M. Beek, MD; Folkert J. ten Cate, MD, PhD;
Jurrien M. ten Berg, MD, PhD; Olga Bondarenko, MD; Marco J.W. Götte, MD, PhD; Jos W.R. Twisk, PhD;
Mark B.M. Hofman, PhD; Cees A. Visser, MD, PhD; Albert C. van Rossum, MD, PhD

Background—Alcohol septal ablation (ASA) reduces left ventricular outflow tract (LVOT) pressure gradient in patients with hypertrophic obstructive cardiomyopathy (HOCM), which leads to left ventricular remodeling. We sought to describe the early to midterm changes and modulating factors of the remodeling process using cardiac MRI (CMR).

Methods and Results—CMR was performed at baseline and 1 and 6 months after ASA in 29 patients with HOCM (age 52 ± 16 years). Contrast-enhanced CMR showed no infarct-related hyperenhancement outside the target septal area. Septal mass decreased from 75 ± 23 g at baseline to 68 ± 22 and 58 ± 19 g ($P<0.001$) at 1- and 6-month follow-up, respectively. Remote, nonseptal mass decreased from 141 ± 41 to 132 ± 40 and 111 ± 27 g ($P<0.001$), respectively. Analysis of temporal trends revealed that septal mass reduction was positively associated with contrast-enhanced infarct size and transmural or left-sided septal infarct location at both 1 and 6 months. Remote mass reduction was associated with infarct location at 6 months but not with contrast-enhanced infarct size. By linear regression analysis, percentage remote mass reduction correlated significantly with LVOT gradient reduction at 6-month follow-up ($P=0.03$).

Conclusions—Left ventricular remodeling after ASA occurs early and progresses on midterm follow-up, modulated by CMR infarct size and location. Remote mass reduction is associated with infarct location and correlates with reduction of the LVOT pressure gradient. Thus, myocardial hypertrophy in HOCM is, at least in part, afterload dependent and reversible and is not exclusively caused by the genetic disorder. (***Circulation.*** 2005;111:2503-2508.)

Key Words: hypertrophy ■ cardiomyopathy ■ ablation ■ remodeling ■ magnetic resonance imaging

In symptomatic patients with hypertrophic obstructive cardiomyopathy (HOCM), alcohol septal ablation (ASA) has been shown to be an attractive alternative to surgical myectomy.[1–4] During the ASA procedure, a chemical infarction is artificially induced, which results in regional thinning of the interventricular septum, an increase in outflow tract diameter, and a decrease in pressure gradient and subsequent symptomatic improvement.[5,6] Some studies have also shown a regression of remote hypertrophy after successful reduction of the outflow tract gradient.[7–11] This may contribute to symptom relief by improving diastolic function.[12] However, reports have not been conclusive, which may be explained in part by the fact that echocardiographic calculations of left ventricular (LV) mass use geometric assumptions that may not be valid in patients with large differences in regional wall thickness. Cardiac MRI (CMR) allows direct mass calculations and has shown high reproducibility in detecting small changes in global and regional mass.[13,14] Using CMR, we recently showed significant reductions in septal and nonseptal, remote myocardial mass 1 month after septal ablation.[15] A progressive reduction in remote mass beyond the early phase would provide strong evidence for the suggested relation between relief of outflow tract gradient and LV remodeling. The aim of this study was therefore to evaluate changes and potential modulating factors of these changes in LV remodeling during the first 6 months after ASA.

Methods

Patients

The study protocol was approved by the Committee on Research Involving Human Subjects and the Medical Ethics Committee of the VU University Medical Center, Amsterdam. Consecutive patients with HOCM scheduled to undergo ASA in 1 of 2 referral centers in the Netherlands were candidates for the study. The indication for ASA was based on a significant LV outflow tract (LVOT) gradient, documented by Doppler echocardiography (≥50 mm Hg), and New

TABLE 1. Patient Characteristics (n=29)

Age, y (men/women)	52±16 (16/13)
NYHA functional class (II/III/IV), n	3.0±0.4 (3/24/2)
Dyspnea/angina/syncope	29/13/5
Medication	
β-Blockers/calcium antagonists	19/16
Antiarrhythmic drugs/diuretics	5/2

Values are expressed as mean±SD (n) or number of patients.

York Heart Association NYHA functional class II, III, or IV despite medical treatment. All patients had basal septal hypertrophy with systolic anterior motion of the anterior mitral valve leaflet. The ASA procedure was described previously.[15] Exclusion criteria were any absolute or relative contraindication to CMR (eg, pacemaker or claustrophobia), atrial fibrillation, or failure to give informed consent. Thirty-three consecutive patients were enrolled initially. Four patients were excluded from the final analysis: 3 required pacemaker implantation because of development of complete atrioventricular block after ASA, and 1 declined to return for the follow-up examinations. The remaining 29 patients formed the final study group. Four patients had resting gradients <50 mm Hg, which increased to ≥50 mm Hg with provocation with the Valsalva maneuver. A successful ablation procedure was defined as >50% gradient reduction at 1 month compared with baseline. The baseline characteristics of these patients are listed in Table 1.

Cardiac MRI

CMR was performed at baseline and 1 and 6 months after ASA with a 1.5-T clinical scanner (Sonata, Siemens) and a 4-element, phased-array body radiofrequency receiver coil. All images were acquired with ECG gating and during repeated breath holds of 10 to 15 seconds, depending on heart rate. Cine images were acquired with a segmented steady state, free precession, gradient-echo sequence in 3 long-axis views (2-, 3-, and 4-chamber view) and in multiple short-axis views every 10 mm, which covered the entire LV from base to apex. At 1-month follow-up, contrast-enhanced CMR was also performed. Contrast-enhanced images were acquired 15 to 20 minutes after intravenous administration of 0.2 mmol/kg gadolinium-DTPA in the same views as in cine CMR with a 2D, segmented, inversion-recovery, prepared gradient-echo sequence.[16–18]

CMR Analysis

Analysis of Contrast-Enhanced Images
Contrast-to-noise ratio of the hyperenhanced area versus a remote nonenhanced myocardial area was measured on the short-axis slice that demonstrated the largest area of hyperenhancement. Contrast-to-noise ratio was calculated with regions of interest and was defined as $(SI_{hyperenhanced} - SI_{remote})$/noise, where SI is signal intensity and noise is expressed as the SI standard deviation in a background region of interest.

Infarct size after ASA was measured by manual tracing of the hyperenhanced area, which was defined as the area within the septal myocardium with pixel SI values >4 SD of remote, nonenhanced myocardium.[15] Central dark zones within the area of hyperenhancement were included. The center of the infarct area was defined as the center of the hyperenhanced area on the short-axis image with the largest area of hyperenhancement.

Analysis of Cine Images
For all patients, CMR scans were placed in random order after the identity markers were removed. Interventricular septal (IVS) wall thickness at the infarct site was measured at end diastole in the short-axis view that included the center of the infarct. The slice position and measurement site was copied from the contrast image to the corresponding cine view of the 1-month study and subsequently to the baseline and 6-month studies. Wall thickness at the septal,

anterior, lateral, and inferior wall and LV end-diastolic and end-systolic dimensions were all determined in the midventricular short-axis view (level of papillary muscles). Left atrial dimension was measured at end systole in the 3- and 4-chamber views. LV end-diastolic volume, end-systolic volume, ejection fraction, and total and septal myocardial mass were quantified with the MASS software package (MEDIS). Endocardial and epicardial borders were outlined manually in end-diastolic and end-systolic frames of all short-axis slices. Papillary muscles were included in the assessment of LV mass. The IVS was defined as the myocardium between the anterior and posterior junctions of the right ventricle to the LV. Remote, nonseptal LV mass was calculated as LV total mass−IVS mass.

Statistical Analysis
Results are expressed as mean±SD. Longitudinal data analysis was performed with generalized estimating equations (GEEs) for serial measurements to evaluate the changes in LV wall thickness, LV end-diastolic and end-systolic dimensions, left atrial dimension, LV volumes, and LV myocardial mass after ASA.[19] In the GEE modeling, time was added as a categorical variable indicated by dummies.[20] In addition to the cru development over time, the influence of certain modulating variables (eg, age, LVOT pressure gradient before ablation, infarct location, and infarct size measured by contrast-enhanced CMR and cardiac enzyme release) was investigated. First, the particular variables were added one at the time to the GEE models to investigate whether the intercept of the development was influenced, ie, whether the variables were stand-alone factors that affected the trend. Second, the interactions between the particular variables and time (ie, the 2-time dummy variables) were added to the models to investigate whether the development over time was different for the different levels of the modulating variables. All GEE analyses were performed with STATA version 7. Linear regression analysis was used to analyze the relationship between LVOT gradient reduction and remote mass reduction. Reproducibility measurements of the acquisition and the intraobserver and interobserver variability (expressed as intraclass coefficients) were calculated in 10 consecutive patients by 2 independent observers. All statistical analyses were performed with SPSS version 11.0, and significance was set at a probability value ≤0.05.

Results
Mean age was 52±16 years (range 18 to 71 years), and 13 of the 29 patients were female. All but one were receiving 1 or more drugs (β-blocker [n=19], calcium channel blockers [n=16], or antiarrhythmic drugs [n=5]). After ASA, the use of medications was reduced markedly (only 10 patients were still taking β-blockers, and 5 of these were receiving half the dosage compared with baseline; only 7 patients were still taking calcium channel blockers). During the ablation procedure, ethanol was injected in 1 septal artery in 27 patients, and 2 septal arteries were ablated in 2 patients. The mean volume of ethanol injected per artery was 3.2±1.5 mL. Before ASA, 25 patients had a resting LVOT pressure gradient ≥50 mm Hg (87±19 mm Hg; range 52 to 120 mm Hg), and 4 had provocable gradients (68±24 mm Hg; range 50 to 100 mm Hg). The mean dynamic pressure gradient decreased from 85±21 to 21±27 mm Hg at 1 month after septal ablation therapy (P<0.01). Four patients had unsuccessful gradient reduction. NYHA functional class improved significantly; at baseline, 3 patients were in NYHA class II, 24 were in class III, and 2 were in class IV. At 1-month follow-up, 13 patients were without symptoms, 12 were in NYHA class II, and 4 were in class III. Three patients were lost for the 6-month follow-up examination: 1 underwent a redo procedure for recurrent symptoms and significant resting
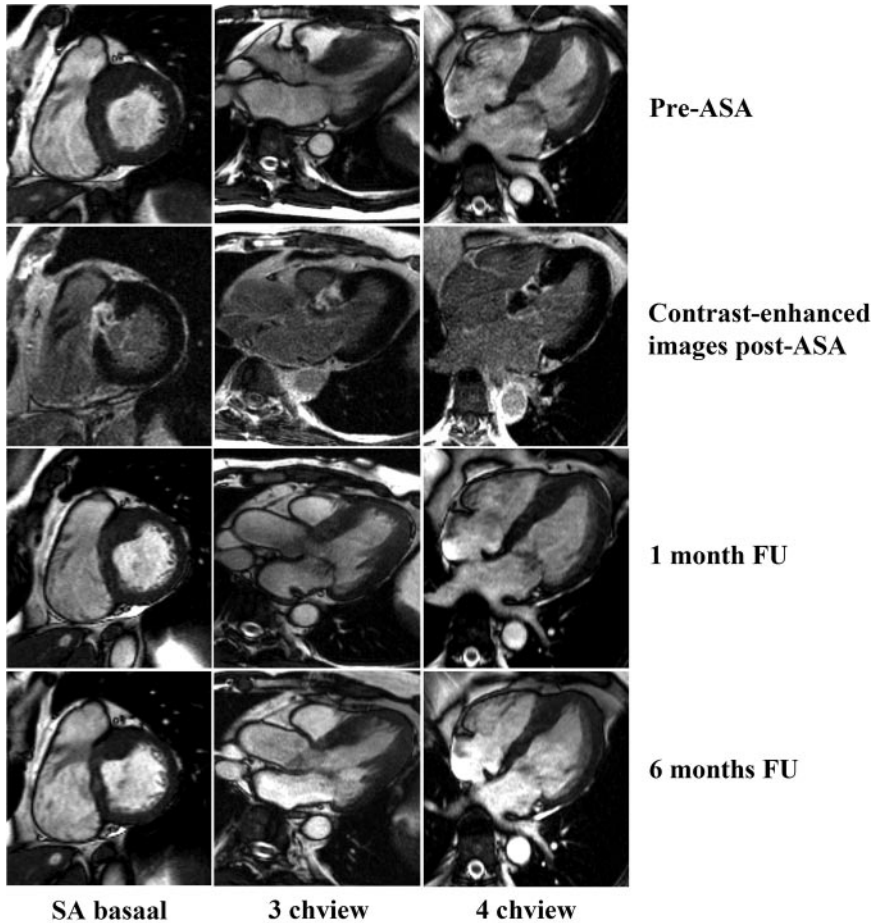
Figure 1. Example of cine and contrast-enhanced magnetic resonance images in patient with HOCM at baseline and at 1 and 6 months after ASA. Distribution of hypertrophy is demonstrated in end-diastolic basal short-axis (SA) view and 3- and 4-chamber views. Thinning of basal interventricular septum is evident, as well as widening of LVOT. Second row demonstrates hyperenhancement in basal septum, which reflects ethanol-induced myocardial infarction 1 month after ASA. FU indicates follow-up; chview, chamber view.

gradient, 1 underwent pacemaker implantation due to late development of complete atrioventricular block after ASA, and 1 had a car accident with multiple bone fractures that made the CMR examination impossible.

Infarct Size and Location
The mean peak creatine kinase (CK) and CK-MB release were 1612 ± 707 U (range 381 to 3366 U) and 217 ± 95 U (range 55 to 371 U), respectively. At 1-month follow-up, a clearly demarcated area of hyperenhancement was visualized in the basal part of the IVS in all patients (Figure 1). Mean myocardial infarct size was 20 ± 9 g (range 5 to 42 g) and involved $11\pm5\%$ of the total LV mass and $32\pm16\%$ of the septal myocardial mass at 1 month after ASA. As we previously reported, the infarct extended transmurally throughout the IVS in 20 patients, was located exclusively on the LV side of the IVS in 2 patients, and was located exclusively on the right ventricular side of the IVS in 7 patients. No patient had evidence of infarct-related hyperenhancement outside the target area.

Changes in LV Wall Thickness and Dimensions
End-diastolic IVS thickness measured at the infarct site decreased from 2.1 ± 0.4 cm at baseline to 1.4 ± 0.4 cm at 1 month and 1.0 ± 0.4 cm at 6 months. Anterior, lateral, and inferior wall thickness at the mid-LV level also progressively decreased at 1 and 6 months after ASA. Whereas LV

end-diastolic dimensions remained unchanged, end-systolic dimensions increased during follow-up. Furthermore, left atrial end-systolic dimensions in both the 3- and 4-chamber views decreased significantly (Table 2).

Longitudinal data analysis of the influence of modulating variables revealed that none influenced the intercept of the development. However, the following modulators affected development over time of the 2D parameters: (1) A larger decrease in IVS wall thickness was associated with a larger contrast-enhanced infarct size ($P<0.01$ at 1 and 6 months, respectively), higher levels of CK ($P<0.01$ and $P=0.06$, respectively) and CK-MB release ($P=0.03$ and $P=0.08$, respectively), and transmural or left-sided septal infarct location ($P<0.01$ at 1 and 6 months, respectively). (2) The decrease in remote myocardial wall thickness was not influenced significantly by any of the variables. (3) A larger increase in LV end-systolic dimension was associated with larger contrast-enhanced infarct size at 1-month follow-up only ($P=0.04$). (4) A larger decrease in left atrial dimension was associated with larger contrast-enhanced infarct size ($P=0.03$) and with transmural or left-sided septal infarct location ($P=0.03$).

Changes in LV Mass, Volumes, and Function
Changes in 3D LV parameters are summarized in Table 3. LV end-diastolic volumes remained unchanged at follow-up, whereas end-systolic volumes increased significantly. Consequently, there was a small decrease in LV ejection fraction at

TABLE 2.   Cardiac Dimensions at Baseline and After ASA

	Baseline	1-Month Follow-Up	6-Month Follow-Up
IVS thickness at infarct site, mm	20.7±4.1	14.5±3.9*	10.2±3.7*
Wall thickness at mid-LV level, mm			
Septal wall	17.5±5.3	16.2±4.8*	14.7±5.0*
Anterior wall	9.6±3.0	9.2±2.9*	8.6±3.1*
Lateral wall	8.2±1.7	7.9±1.7*	7.1±1.6*
Inferior wall	10.2±2.9	9.7±2.8*	9.3±2.8*
LV end-diastolic diameter, mm	47.8±5.3	47.8±5.8	47.5±5.7
LV end-systolic diameter, mm	25.8±4.0	29.3±6.0*	28.8±5.7*
LA end-systolic diameter (3-chamber view), mm	50.9±6.5	46.2±6.8*	45.7±7.2*
LA end-systolic diameter (4-chamber view), mm	59.2±7.4	54.5±6.3*	52.4±5.8*

Values are expressed as mean±SD.

*$P<0.01$ vs baseline.

1 and 6 months. Total LV myocardial mass decreased from 216±62 g at baseline to 200±60 g (−8%) at 1 month and 170±45 g (−21%) at 6 months. Septal myocardial mass decreased from 75±23 to 68±22 g (−10%) at 1 month and to 58±19 g (−23%) at 6 months. Nonseptal mass decreased from 141±41 g at baseline to 132±40 g (−6%) at 1 month and to 111±27 g (−21%) at 6 months' follow-up. The relative reduction of septal and nonseptal myocardial mass is shown in Figure 2.

Also with respect to these 3D parameters, the intercept of the development was not influenced by the modulating variables. Time-dependent trends were as follows: (1) A larger decrease of septal mass was associated with larger contrast-enhanced infarct size ($P<0.01$ at 1 and 6 months, respectively), higher levels of CK ($P=0.05$ at 1 month and $P<0.01$ at 6 months) and CK-MB ($P=0.17$ at 1 month and $P=0.03$ at 6 months), and transmural or left-sided septal location ($P<0.01$ at 1 and 6 months, respectively). (2) A larger decrease of remote mass was associated with transmural or left-sided septal infarct location ($P=0.12$ at 1 month and $P<0.01$ at 6 months) but not with contrast-enhanced septal infarct size.

Reproducibility measurements of image acquisition and intraobserver and interobserver variability were performed in 10 consecutive patients by 2 independent observers. Intraclass coefficients of reproducibility and of intraobserver and interobserver variability ranged between 0.98 and 0.99 for end-diastolic volume, end-systolic volume, ejection fraction, and myocardial mass, respectively.

Correlation Between Regional Mass Reduction and Gradient Reduction

Linear regression analysis showed a significant association between percent reduction of remote mass and LVOT pressure gradient reduction at 6-month follow-up ($r=0.44$, $P=0.03$; Figure 3). No correlation was found between percent reduction of septal mass and LVOT gradient reduction ($r=0.31$, $P=0.12$).

Discussion

Quantitative analysis without geometric assumptions revealed a significant early and progressive LV remodeling with reduction in septal and remote myocardial mass throughout the 6-month follow-up period. Whereas diastolic volumes remained unchanged, systolic volumes increased, and left atrial dimensions decreased. CMR-derived infarct size and location were found to modulate the early temporal changes of the parameters that reflect the LV remodeling process. Whereas reduction in septal mass was associated with infarct size and location, reduction in remote mass was associated with infarct location and not with infarct size and correlated significantly with reduction of the LVOT gradient. Because absence of hyperenhancement outside the target septal area excluded alcohol-induced injury on remote myocardium, remote myocardial remodeling may be attributed to the reduction in outflow tract gradient and the concomitant decrease in LV wall stress. The association with infarct location became apparent at 6 months only, which reflects a

TABLE 3.   LV Volumes and Mass at Baseline and After ASA

	Baseline	1-Month Follow-Up	6-Month Follow-Up
LV end-diastolic volume, mL	170±42	167±41	169±39
LV end-systolic volume, mL	54±16	57±18*	59±17†
Stroke volume, mL	116±29	110±25*	110±25
LV ejection fraction, %	69±5	67±5†	66±4†
Total LV mass, g	216±62	200±60†	170±45†
Septal mass, g	75±23	68±22†	58±19†
Nonseptal mass, g	141±41	132±40†	111±27†

Values are expressed as mean±SD.

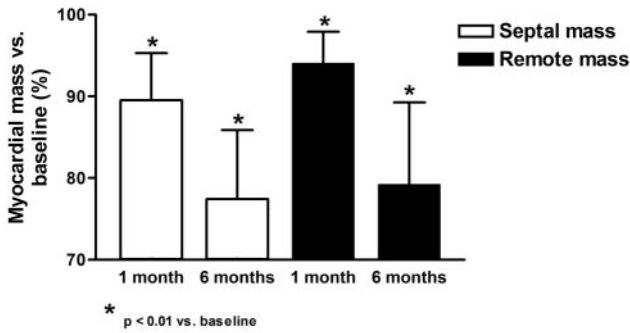*$P<0.05$ vs baseline; †$P<0.01$ vs baseline.

Figure 2. Percent changes in septal and remote LV myocardial mass after ASA at 1- and 6-month follow-up.

more gradual process of remodeling than in the IVS, where the association is immediately apparent at 1 month and remains at 6 months because of the directly inflicted infarct. Also, the reversibility of the remote myocardial mass implies that hypertrophy in HOCM is not caused exclusively by the genetic disorder but is induced, at least in part, secondary to the dynamic obstruction of the outflow tract.

Changes in Septal and Remote Myocardial Mass After ASA

The genetic disorder in HOCM leads to a primary molecular abnormality. Expression of mutant sarcomeric proteins (contractile units) leads to a decrease in generation of force, which results in impaired cardiac myocyte contractility and increased cardiac myocyte stress.[21] In the subset of patients with LVOT obstruction, increased LV pressure and wall stress induce secondary hypertrophy that may be (partly) reversible after elimination of the LVOT obstruction.[9,22] Previous echocardiographic studies have shown ambiguous results with respect to reduction of LV posterior wall thickness.[7–11,23–26] Tomographic techniques such as electron-beam

Figure 3. Correlation between reduction in remote myocardial mass and LVOT gradient reduction at 6-month follow-up.

computed tomography and CMR may be more accurate and reproducible than echocardiographic measurements and LV mass calculations. Electron-beam computed tomography showed septal mass reduction 1 week after ASA and found reduced remote mass at 4 to 6 months of follow-up.[11] The results of the present study using CMR are in line with these observations and additionally revealed factors associated with the remodeling process over time. Not surprisingly, septal wall thickness and septal mass demonstrated immediate and progressive reduction associated with the alcohol-induced infarct size and location at 1 and 6 months. Reduction of remote wall thickness, however, although significant at 1 and 6 months, was not associated with infarct size and location at any time, whereas reduction of the mass did show an association with infarct location at 6 months. 2D measurements of wall thickness performed regionally probably are less precise than 3D mass calculation of the entire remote myocardium in revealing the association with the gradual process of remote remodeling over time.

The early onset of regression of remote hypertrophy may be explained by an immediate reduction in the expression of cardiac growth factors. Nagueh et al[22] found decreased expression of myocardial tumor necrosis factor-α in patients with HOCM 6 weeks after relief of the LVOT obstruction by ASA. The decreased cardiac levels of tumor necrosis factor-α were accompanied by a reduction in myocyte size and in the amount of interstitial collagen.

The causative relation between regression of remote hypertrophy and reduction in outflow tract gradient is supported by the correlation that reached statistical significance at 6-month follow-up. The relation between septal mass reduction and outflow tract gradient reduction was not significant. Septal mass reduction is the result of the chemically induced infarction and subsequent scar formation, a direct process that is not secondary to the reduction in LVOT gradient. This is supported by the positive time-dependent interactions of septal mass reduction with contrast-enhanced infarct size: a larger reduction in septal myocardial mass was associated with larger contrast-enhanced infarcts. In contrast, the change in remote mass was not associated with contrast-enhanced infarct size but only with transmural or left-sided septal location.
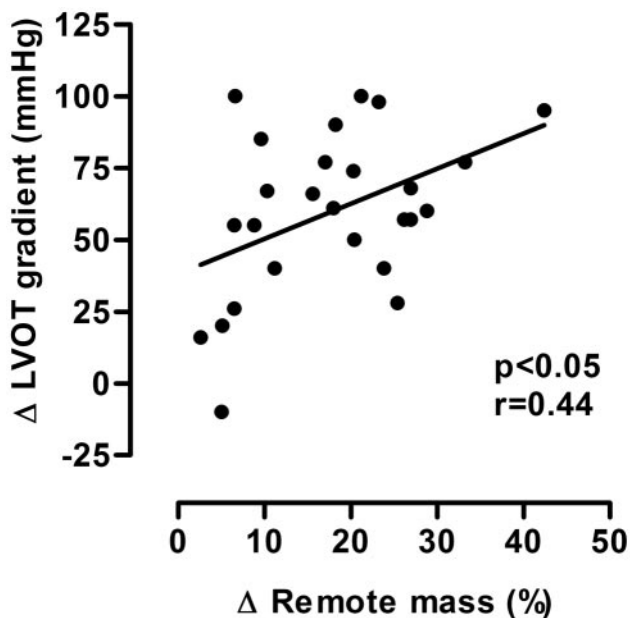
Changes in Dimensions and Volumes After ASA
Previous studies have generally found significant increases in both end-systolic and end-diastolic dimensions.[9,27] We found a significant increase in end-systolic dimension and a small but significant increase in LV end-systolic volume at 6-month follow-up. These changes may be explained by septal thinning and reduced thickening as a result of the ethanol-induced infarction. LV end-diastolic dimension and volume remained unchanged at both follow-up CMR scans. As a result, there was a small decrease in LV ejection fraction at 6 months.

Left atrial dimensions decreased after ASA, with larger decreases being associated with larger contrast-enhanced infarcts. The decrease is likely to reflect the effect of the ASA procedure on improving diastolic function.

A general limitation of the present study is the difficulty in obtaining blinded measurements, because effects of treatment

by ASA are often clearly visible for the experienced CMR observer, which thus introduces observer bias in judgment of postablation wall thickness. In the present study, we did not measure the increase in LVOT area, which has been shown to have a close relationship with the decrease in septal wall thickness.[28] These measurements, however, require imaging of the LVOT in multiple orientations, with addition of flow quantification acquisitions, which is time consuming. In our imaging protocol, we gave priority to the addition of acquisitions of delayed imaging after gadolinium. Furthermore, only left atrial dimensions were measured, which are likely to be less accurate than volume determinations. However, our primary aim was not to measure the effects of ASA on left atrial volumes, and consequently, the CMR protocol did not include full coverage for measuring left atrial volume. We merely sought to provide circumstantial evidence in support of improvement of diastolic function. Moreover, dimensions may be more meaningful to clinicians than left atrial volumes.

In summary, we used CMR to evaluate LV remodeling after ASA in symptomatic patients with HOCM. LV remodeling occurred early and progressed on midterm follow-up, modulated by infarct size and location. Regression of non-septal, remote myocardial mass was significantly associated with infarct location and correlated with the reduction in LVOT pressure gradient at 6-month follow-up. Our findings support the theory that myocardial hypertrophy in patients with HOCM is, at least in part, afterload dependent and reversible and thus is not caused exclusively by the genetic disorder.

Acknowledgment

References

1. Sigwart U. Non-surgical myocardial reduction for hypertrophic obstructive cardiomyopathy. *Lancet*. 1995;346:211–214.
2. Knight C, Kurbaan AS, Seggewiss H, Henein M, Gunning M, Harrington D, Fassbender D, Gleichmann U, Sigwart U. Nonsurgical septal reduction for hypertrophic obstructive cardiomyopathy: outcome in the first series of patients. *Circulation*. 1997;95:2075–2081.
3. Seggewiss H, Gleichmann U, Faber L, Fassbender D, Schmidt HK, Strick S. Percutaneous transluminal septal myocardial ablation in hypertrophic obstructive cardiomyopathy: acute results and 3-month follow-up in 25 patients. *J Am Coll Cardiol*. 1998;31:252–258.
4. Lakkis NM, Nagueh SF, Kleiman NS, Killip D, He Z-X, Verani MS, Roberts R, Spencer WH III. Echocardiography-guided ethanol septal reduction for hypertrophic obstructive cardiomyopathy. *Circulation*. 1998;98:1750–1755.
5. Fananapazir L, McAreavey D. Therapeutic options in patients with obstructive hypertrophic cardiomyopathy and severe drug-refractory symptoms. *J Am Coll Cardiol*. 1998;31:259–264.
6. Roberts R, Sigwart U. New concepts in hypertrophic cardiomyopathies, part II. *Circulation*. 2001;104:2249–2252.
7. Faber L, Seggewiss H, Gleichmann U. Percutaneous transluminal septal myocardial ablation in hypertrophic obstructive cardiomyopathy: results with respect to intraprocedural myocardial contrast echocardiography. *Circulation*. 1998;98:2415–2421.
8. Faber L, Meissner A, Ziemssen P, Seggewiss H. Percutaneous transluminal septal myocardial ablation for hypertrophic obstructive cardiomyopathy: long term follow up of the first series of 25 patients. *Heart*. 2000;83:326–331.
9. Mazur W, Nagueh SF, Lakkis NM, Middleton KJ, Killip D, Roberts R, Spencer WH III. Regression of left ventricular hypertrophy after nonsurgical septal reduction therapy for hypertrophic obstructive cardiomyopathy. *Circulation*. 2001;103:1492–1496.
10. Lakkis N, Plana JC, Nagueh S, Killip D, Roberts R, Spencer WH III. Efficacy of nonsurgical septal reduction therapy in symptomatic patients with obstructive hypertrophic cardiomyopathy and provocable gradients. *Am J Cardiol*. 2001;88:583–586.
11. Boekstegers P, Steinbigler P, Molnar A, Schwaiblmair M, Becker A, Knez A, Haberl R, Steinbeck G. Pressure-guided nonsurgical myocardial reduction induced by small septal infarctions in hypertrophic obstructive cardiomyopathy. *J Am Coll Cardiol*. 2001;38:846–853.
12. Nagueh SF, Lakkis NM, Middleton KJ, Killip D, Zoghbi WA, Quiñones MA, Spencer WH III. Changes in left ventricular diastolic function 6 months after nonsurgical septal reduction therapy for hypertrophic obstructive cardiomyopathy. *Circulation*. 1999;99:344–347.
13. Mogelvang J, Lindvig K, Sondergaard L, Saunamaki K, Henriksen O. Reproducibility of cardiac volume measurements including left ventricular mass determined by MRI. *Clin Physiol*. 1993;13:587–597.
14. Myerson SG, Bellenger NG, Pennell DJ. Assessment of left ventricular mass by cardiovascular magnetic resonance. *Hypertension*. 2002;39:750–755.
15. van Dockum WG, ten Cate FJ, ten Berg JM, Beek AM, Twisk JWR, Vos J, Hofman MBM, Visser CA, van Rossum AC. Myocardial infarction after percutaneous transluminal septal myocardial ablation in hypertrophic obstructive cardiomyopathy: evaluation by contrast-enhanced magnetic resonance imaging. *J Am Coll Cardiol*. 2004;43:27–34.
16. Wu E, Judd RM, Vargas JD, Klocke FJ, Bonow RO, Kim RJ. Visualization of presence, location, and transmural extent of healed Q-wave and non-Q-wave myocardial infarction. *Lancet*. 2001;357:21–28.
17. Simonetti OP, Kim RJ, Fieno DS, Hillenbrand HB, Wu E, Bundy JM, Finn JP, Judd RM. An improved MR imaging technique for the visualization of myocardial infarction. *Radiology*. 2001;218:215–223.
18. Kim RJ, Shah DJ, Judd RM. How we perform delayed enhancement imaging. *J Cardiovasc Magn Reson*. 2003;5:505–514.
19. Diggle PJ, Heagerty PJ, Liang KY, Zeger SL. *Analysis of Longitudinal Data*. 2nd ed. New York, NY: Oxford University Press; 2002.
20. Twisk JWR. *Applied Longitudinal Data Analysis for Epidemiology: A Practical Guide*. Cambridge, UK: Cambridge University Press; 2003.
21. Marian AJ. Pathogenesis of diverse clinical and pathological phenotypes in hypertrophic cardiomyopathy. *Lancet*. 2000;355:58–60.
22. Nagueh SF, Stetson SJ, Lakkis NM, Killip D, Perez-Verdia A, Entman ML, Spencer WH III, Torre-Amione G. Decreased expression of tumor necrosis factor-α and regression of hypertrophy after nonsurgical sepal reduction therapy for patients with hypertrophic obstructive cardiomyopathy. *Circulation*. 2001;103:1844–1850.
23. Henein MY, O'Sullivan CA, Ramzy IS, Sigwart U, Gibson DG. Electromechanical left ventricular behavior after nonsurgical septal reduction in patients with hypertrophic obstructive cardiomyopathy. *J Am Coll Cardiol*. 1999;34:1117–1122.
24. Lakkis NM, Nagueh SF, Dunn JK, Killip D, Spencer WH III. Nonsurgical septal reduction therapy for hypertrophic obstructive cardiomyopathy: one year follow-up. *J Am Coll Cardiol*. 2000;36:852–855.
25. Qin JX, Shiota T, Lever HM, Kapadia SR, Sitges M, Rubin DN, Bauer F, Greenberg NL, Agler DA, Drinko JK, Martin M, Tuzcu EM, Smedira NG, Lytle B, Thomas JD. Outcome of patients with hypertrophic obstructive cardiomyopathy after percutaneous transluminal septal myocardial ablation and septal myectomy surgery. *J Am Coll Cardiol*. 2001;38:1994–2000.
26. Veselka J, Honek T. Early remodeling of left ventricle and improvement of myocardial performance in patients after percutaneous transluminal septal myocardial ablation for hypertrophic obstructive cardiomyopathy. *Int J Cardiol*. 2002;88:27–32.
27. Sitges M, Shioto T, Lever HM, Qin JX, Bauer F, Drinko J, Agler DA, Martin MG, Greenberg NL, Smedira NG, Lytle B, Tuzcu EM, Garcia MJ, Thomas JD. Comparison of left ventricular diastolic function in obstructive hypertrophic cardiomyopathy in patients undergoing percutaneous septal alcohol ablation versus surgical myotomy/myectomy. *Am J Cardiol*. 2003;91:817–821.
28. Schulz-Menger J, Strohm O, Waigand J, Uhlich F, Dietz R, Friedrich MG. The value of magnetic resonance imaging of the left ventricular outflow tract in patients with hypertrophic obstructive cardiomyopathy after septal artery embolization. *Circulation*. 2000;101:1764–1766.